行政院國家科學委員會專題研究計畫 期中進度報告

用於增進MIMO-OFDM 系統性能之編碼與調變--子計畫二：具低均峰比率及錯誤率之MIMO OFDM系統(1/3)
期中進度報告(完整版)

計 畫 類 別 ：整合型
計 畫 編 號 ：NSC 95-2219-E-002-026-
執 行 期 間 ：95年08月01日至96年07月31日
執 行 單 位 ：國立臺灣大學電機工程學系暨研究所

計 畫 主 持 人 ：林茂昭

處 理 方 式 ：期中報告不提供公開查詢

中 華 民 國 96年05月25日

用於增進 MIMO-OFDM 系統性能之編碼與調變-子計畫:二具低均峰比率及錯誤率之 MIMO OFDM 系統(1/3)

MIMO OFDM Systems with Low PAPR and Error rates(1/3)

計畫編號　：　NSC 95-2219-E-002-026
執行期限　：　95/08/01 ~ 96/7/31
計畫主持人　：　林茂昭

摘要 —

在多輸入多輸出正交分頻多工系統中，空頻碼已經有廣泛的研究與討論。在這篇報告中，在兩根傳送天線的情形下，我們討論的空頻碼是把低密度同位檢查碼與阿拉姆提碼串連連結而成。也基於此種空頻碼，我們提出一種如何簡單的降低峰均值功率比之技術。因爲這個技術只需在時域上做運算，而不須要在頻域上來做運算，因此傳統上使用選擇性對應技術時，會有反向離散快速傅立葉轉換計算量很大的缺點，但在此技術下會大量的減低到只需要兩個。此提出的技術用在較少的候選數目時會比較優良，不但可以簡化系統而且也不會犧牲掉錯誤率，這些結果最後都會用電腦把它模擬出來。

關鍵詞 **— 空頻碼，峰均值功率比，時域，低密度同位檢查碼，阿拉姆提碼**

Abstract

We consider the problem of space-frequency (SF) codes design for multiple-input-multiple-output (MIMO) orthogonal frequency division multiplexing (OFDM) modulation in frequency-selective Rayleigh fading channel. In particular, we investigate a space-frequency code with two transmit antennas that is constructed by the concatenation of binary LDPC code and the Alamouti space-time coding. Based on this efficient space-frequency code, we propose a low complexity selective-mapping type PAPR reduction technique. In the proposed technique, the candidates are generated in the time-domain instead of the frequency domain. Thus, only two IFFT operations are needed in the proposed technique while for the selective mapping using frequency domain many IFFT operations are needed. In case the number of candidates is not great (no more than 16), the proposed technique can significantly reduce the complexity without sacrificing the PAPR reduction capability and error rates. Simulation results verify the advantage of the proposed PAPR reduction technique.

Index Term **–Alamouti code, Low-density parity-check (LDPC) codes, peak-to-average power ratio, space-frequency codes, time domain.**

Contents

List of Tables

List of Figures

Chapter 1

INTRODUCTION

It has been well recognized that Multiple-input-multiple-output (MIMO) systems employing multiple transmit and receive antennas can play a significant role in the broadband wireless communications. By employing the diverse characteristics of channels between each pair of transmit and receive antennas, the MIMO system can provide a large potential capacity increase as compared with the conventional single antenna systems. To exploit this capacity increase, many *space-time* (ST) codes have been proposed, such as [1, 2, 3, 4, 5, 6]. These ST codes were basically designed for flat fading channels. In case of broadband wireless communication systems, the channels are frequency selective channel, resulting in inter symbol interference (ISI)[7]. Orthogonal frequency division multiplexing (OFDM) is a technique, which is effective in combating the problem of ISI. [8].

In order to combine the advantages of both the MIMO systems and the OFDM, *space-frequency* (SF) coded MIMO-OFDM systems have been proposed [9], where two-dimensional coding is applied to distribute channel symbols across space (transmit antennas) and frequency (OFDM tones). In [10], an SF coding was obtained by exchanging the time domain arrangement for the frequency domain arrangement in the existing ST coding.

In the ST coding, the achievable diversity advantage is bounded by the product of the number of transmit antennas and the number of receive antennas [2]. Usually, multiple delayed paths will deteriorate the error performance in the digital transmission. However, SF codes can turn the negative effect of multiple delayed paths into advantage. In fact, SF coding can have additional *multipath* diversity in case the transmission is over the frequency-selective fading channel. Using SF coding, the maximum diversity is product of the number of transmit antennas, the number of receive antennas and the number of channel delay paths [9].

A well known problem for the OFDM system is the occasionally occurred high peak-to-average power ratio (PAPR), that is due to its approximately Gaussian distributed output signal samples. An OFDM system with high PAPR requires a costly linear power amplifier with large dynamic range for the transmitter, otherwise significant out-of-band energy and signal distortion will occur. By now, many techniques

have been proposed for relieving the PAPR problem in the OFDM, such as Amplitude Clipping, Coding, Selective Mapping (SLM) [11, 12] and Active Constellation Extension (ACE) [13]. For MIMO OFDM, the problem of PAPR is similar to the conventional OFDM system. The techniques used for mitigating the PAPR effect in the conventional OFDM system can also be applied to the MIMO OFDM systems. However, the usage of multiple transmit antennas may somewhat deepen the problem of PAPR while also may provide additional room for executing the operation of PAPR reduction.

In this first-year report of the three-year project, we have completed the investigation of an efficient MIMO-OFDM system, which is constructed by the concatenation of LDPC coding and Alamouti coding. By insuring the good error performance of this concatenated SF code, we further investigate the associated PAPR problem. We propose a low-complexity PAPR reduction technique for the investigated SF code, which is a kind of selective mapping technique implemented on the time-domain. Compared to a known PAPR reduction technique for MIMO-OFDM [14] that is a selective mapping technique implemented on the frequency domain, the proposed PAPR reduction technique is more effective in PAPR reduction in case the number of candidates is not large, even though the proposed technique has lower complexity.

This report is organized as follows. The review of some MIMO-OFDM properties is given in Chapter 2. The SF code constructed from the concatenation of a binary

LDPC code and the Alamouti code and its related performances are described in Chapter 3. In Chapter 4, a new PAPR reduction technique for SF codes is shown. Finally, Conclusions are given in Chapter 5.

Chapter 2

SYSTEM MODEL

2.1 Space-Time Codes

Throughout this report, we consider the MIMO system with N_t transmit antennas and N_r receive antennas signaling over the fading channel. The received signal at time t ($t = 1, 2, \cdots, T$) at the jth receive antenna ($j = 1, 2, \ldots, N_r$) is given by

$$r_j(t) = \sqrt{\frac{E_s}{N_t}} \sum_{i=1}^{N_t} h_{j,i}(t) s_i(t) + n_j(t). \tag{2.1}$$

where $s_i(t)$ is the symbol transmitted from the ith transmit antenna at time t, $h_{j,i}$ is the complex fading gain from the ith transmit antenna to receive jth receive antenna, and $n_j(t)$ denotes the additive complex Gaussian noise with zero mean and unit variance at time t. The received signal in Eqs.(2.1) can be rewritten in matrix form

as

$$R = \sqrt{\frac{E_s}{N_t}} HS + N. \tag{2.2}$$

where R, H, N and S are respectively

$$R = \begin{bmatrix} R_{11} & R_{12} & \cdots & R_{1T} \\ R_{21} & R_{22} & \cdots & R_{2T} \\ \vdots & \vdots & \ddots & \vdots \\ R_{N_r1} & R_{N_r2} & \cdots & R_{N_rT} \end{bmatrix}, \quad H = \begin{bmatrix} H_{11} & H_{12} & \cdots & H_{1N_t} \\ H_{21} & H_{22} & \cdots & H_{2N_t} \\ \vdots & \vdots & \ddots & \vdots \\ H_{N_r1} & H_{N_r2} & \cdots & H_{N_rN_t} \end{bmatrix} \tag{2.3}$$

$$N = \begin{bmatrix} N_{11} & N_{12} & \cdots & N_{1T} \\ N_{21} & N_{22} & \cdots & N_{2T} \\ \vdots & \vdots & \ddots & \vdots \\ N_{N_r1} & N_{N_r2} & \cdots & N_{N_rT} \end{bmatrix}, \quad S = \begin{bmatrix} s_{11} & s_{12} & \cdots & s_{1T} \\ s_{21} & s_{22} & \cdots & s_{2T} \\ \vdots & \vdots & \ddots & \vdots \\ s_{N_t1} & s_{N_t2} & \cdots & s_{N_tT} \end{bmatrix} \tag{2.4}$$

The matrix S represents a codeword of the space time code. The ith row of S is composed of the symbols transmitted from the ith transmit antenna over a period of T. The jth column of S is composed of the symbols transmitted from all the N_t antennas at the jth time slot.

2.2 Space-Frequency (SF) Codes

For a space time code, its codeword consists of symbols transmitted from all the N_t antennas over a period of time. In contrast, for a space frequency code, its codeword consists of symbols transmitted from all the N_t antennas over a frequency band comprising many subcarriers.

2.2.1 System Model

Consider an SF-coded MIMO-OFDM system with N_t transmit antennas, N_r receive antennas, and K subcarriers. Suppose that all the frequency-selective fading channels, each represents a pair of transmit antenna and receive antenna, have L independent delay paths and the same power delay profile. The MIMO channel is assumed to remain unchanged over the period of each OFDM block. The channel impulse response from the ith transmit antenna to the jth receive antenna can be modelled as

$$h_{j,i}(\tau) = \sum_{l=0}^{L-1} \alpha_{j,i}(l)\delta(\tau - \tau_l). \tag{2.5}$$

where τ_l is the delay of the lth path, and $\alpha_{j,i}(l)$ is the complex amplitude of the lth path between transmit antenna i to receive antenna j. Each $\alpha_{j,i}(l)$ is a complex Gaussian random variable with zero mean and variances $E|\alpha_{j,i}(l)|^2 = \delta_l^2$, where E stands for the operation of expectation. Note that the time delay τ_l and the variance

δ_l^2 are the same for all the pairs represented by (i, j), $i = 1, 2, \cdots, N_t$, $j = 1, 2, \cdots, N_r$. The variances of the L paths are normalized such that $\sum_{l=0}^{L-1} \delta_l^2 = 1$. From Eqs.(2.5), the frequency response of the channel represents the pair (i, j) is given by

$$H_{j,i}(f) = \sum_{l=0}^{L-1} \alpha_{j,i}(l) e^{-\mathbf{j}\, 2\pi f \tau_l}, \quad \mathbf{j} = \sqrt{-1}. \tag{2.6}$$

We assume that the MIMO channel is spatially uncorrelated, i.e., all the $\alpha_{j,i}(l)$'s are statistically independent. The space frequency codeword can be expressed as an $Nt \times K$ matrix

$$C = \begin{bmatrix} c_1(0) & c_1(1) & \dots & c_1(K) \\ c_2(0) & c_2(1) & \dots & c_2(K) \\ \vdots & \vdots & \ddots & \vdots \\ c_{N_t}(0) & c_{N_t}(1) & \dots & c_{N_t}(K) \end{bmatrix} \tag{2.7}$$

where $c_i(k)$ denotes the channel symbol transmitted over kth subcarrier by transmit antenna i. Each space frequency codeword is assumed to satisfy the energy constraint of $E[\|C\|_F^2] = N_t K$, where $\|C\|_F$ is the Frobenius norm [1] of C.

The OFDM transmitter applies a K-point IFFT (inverse fast Fourier transform) to each row of the matrix C. After appending a cyclic prefix (CP), the OFDM symbol corresponding to the ith row of C is transmitted by the ith transmit antenna. At the receiver, after matched filtering, removing the CP, and applying FFT, the received

[1] The *matrix norm* of an $m \times n$ matrix A is defined as the square root of the sum of the absolute squares of its elements.

signal at the kth subcarrier at the jth receive antenna is given by

$$y_j(k) = \sqrt{\frac{E_s}{N_t}} \sum_{i=1}^{N_t} H_{j,\,i}(k) c_i(k) + n_j(k). \tag{2.8}$$

where

$$H_{j,i}(k) = \sum_{l=0}^{L-1} \alpha_{j,\,i}(l) e^{-\mathbf{j}\,2\pi k \Delta f \tau_l}. \tag{2.9}$$

is the channel frequency response at the nth subcarrier between the ith transmit antenna and the jth receive antenna, $\Delta f = 1/T$ is the subcarrier separation in the frequency domain, and T is the OFDM symbol period. Let

$$\Lambda_{j,i} = \left[\begin{array}{cccc} \alpha_{j,\,i}(1) & \alpha_{j,\,i}(2) & \cdots & \alpha_{j,\,i}(L) \end{array} \right]^H \tag{2.10}$$

$$\omega_k = \left[\begin{array}{cccc} e^{-\mathbf{j}\,2\pi k \Delta f \tau_1} & e^{-\mathbf{j}\,2\pi k \Delta f \tau_2} & \ldots & e^{-\mathbf{j}\,2\pi k \Delta f \tau_L} \end{array} \right]^T \tag{2.11}$$

Eqs.(2.9) can be written as

$$H_{j,i}(k) = (\Lambda_{j,i})^H \omega_k \tag{2.12}$$

We assume that the CSI (channel state information), $H_{j,i}(k)$, is known at the receiver. In Eqs.(2.8), $n_j(k)$ denotes the additive complex Gaussian noise with zero mean and unit variance at the kth subcarrier at the jth receive antenna. The noise samples $n_j(k)$'s are assumed to be uncorrelated for different j and k. Using the factor $\sqrt{E_s/N_t}$ in Eqs.(2.8) can ensure that E_s is the average SNR at each receive antenna

and is independent of the number of transmit antennas.

2.2.2 Design Criteria

Consider the maximum likelihood decoding [15, 16] of the space frequency code by

$$\hat{C} = \arg\min_{\hat{C}} \sum_{j=1}^{N_r} \sum_{k=1}^{K} \left| y_j(k) - \sum_{i=1}^{N_t} H_{j,i}(k) c_i(k) \right|^2 \tag{2.13}$$

where the minimization is performed over all possible space frequency codewords. Let $d_H^2(C, \hat{C})$ be described as

$$\begin{aligned} d_H^2(C, \hat{C}) &= \sum_{j=1}^{N_r} \sum_{k=1}^{K} \left| \sum_{i=1}^{N_t} H_{j,i}(k)[c_i(k) - \hat{c}_i(k)] \right|^2 && (2.14) \\ &= \sum_{j=1}^{N_r} \sum_{k=1}^{K} \left| \sum_{i=1}^{N_t} (\Lambda_{j,i})^H \omega_k [c_i(k) - \hat{c}_i(k)] \right|^2 && (2.15) \\ &= \sum_{j=1}^{N_r} \sum_{k=1}^{K} | \Gamma_j W_k e_k|^2 && (2.16) \end{aligned}$$

where Eqs.(2.15) is derived from Eqs.(2.12) and in Eqs.(2.16), the new matrix Γ_j,W_k and e_k are shown below

$$\begin{aligned}
\Gamma_j &= \begin{bmatrix} (\Lambda_{j,1})^H & (\Lambda_{j,2})^H & \cdots & (\Lambda_{j,N_t})^H \end{bmatrix}_{1\times LN_t} \\
W_k &= \begin{bmatrix} w_k & 0 & \cdots & 0 \\ 0 & w_k & \cdots & 0 \\ \vdots & \vdots & \ddots & \vdots \\ 0 & 0 & \cdots & w_k \end{bmatrix}_{LN_t\times N_t} \\
e_k &= \begin{bmatrix} c_1(k) - \hat{c}_1(k) \\ c_2(k) - \hat{c}_2(k) \\ \vdots \\ c_{N_t}(k) - \hat{c}_{N_t}(k) \end{bmatrix}_{N_t\times 1}
\end{aligned} \tag{2.17}$$

Assuming that perfect CSI is available at the receiver, the pairwise error probability of the transmitted codeword C and the erroneously decoded codeword $\hat{C}$ conditioned on a fixed H is given by

$$P(C,\hat{C}|H) \leq \exp\left(-d_H^2(C,\hat{C})\frac{E_s}{4N_0}\right) \tag{2.18}$$

where E_s is the average symbol energy, N_0 is the one-sided power spectral density of the additive white Gaussian noise (AWGN).

Eqs.(2.16) can be written as

$$\begin{aligned} d_H^2(C,\hat{C}) &= \sum_{j=1}^{N_r}\sum_{k=1}^{K}\left(\,\Gamma_j W_k e_k e_k^H W_k^H \Gamma_j^H\right) \\ &= \sum_{j=1}^{N_r}\,\Gamma_j\left(\sum_{k=1}^{K} W_k e_k e_k^H W_k^H\right)\Gamma_j^H \\ &= \sum_{j=1}^{N_r}\,\Gamma_j D_H(C,\hat{C})\Gamma_j^H \end{aligned} \tag{2.19}$$

where $D_H(C,\hat{C})$ is an $LN_t \times LN_t$ matrix given by

$$D_H(C,\hat{C}) = \sum_{k=1}^{K} W_k e_k e_k^H W_k^H \tag{2.20}$$

Note that the matrix $D_H(C,\hat{C})$ is concerned about the codeword difference and the power delay profile of the channels. Denote the rank of $D_H(C,\hat{C})$ by γ. In Eqs.(2.20), we know $rank(e_k e_k^H) = 1$ if and only if e_k is not a zero vector, otherwise, $rank(e_k e_k^H) = 0$. Assume the number of nonzero vector in $e_1, e_2, \ldots, e_K$ is $\widehat{\gamma}$. Thus, $D_H(C,\hat{C})$ is the sum of $\widehat{\gamma}$ rank one matrices. It can be derived that

$$rank(D_H(C,\hat{C})) = \gamma \leq \min(\widehat{\gamma}, LN_t) \leq \min(K, LN_t). \tag{2.21}$$

since $\widehat{\gamma} \leq K$. For the nonnegative definite Hermitian matrix $D_H(C,\hat{C})$, its eigenvalues can be ordered as

$$\lambda_1 \geq \lambda_2 \geq \ldots \geq \lambda_\gamma > 0 \tag{2.22}$$

By averaging Eqs.(2.18) with respect to the channel H, the pairwise error probability can be derived from [17] as

$$P(C, \hat{C}) \leq \left(\prod_{j=1}^{\gamma} \lambda_j \right)^{-N_r} \left(\frac{E_s}{4N_0} \right)^{-\gamma N_r} \tag{2.23}$$

Thus, the maximum achievable diversity is at most $\min(KN_r, LN_tN_r)$. As a consequence, we can formulate the performance criteria as follows

- *Diversity (rank) criterion*: The minimum rank of $D_H(C, \hat{C})$, i.e., γ, over all pairs of distinct signals C and $\hat{C}$ should be as large as possible.

- *Product criterion*: The minimum value of the product $\prod_{j=1}^{\gamma} \lambda_j$ over all pairs of distinct signals C and $\hat{C}$ should also be maximized.

Chapter 3

LDPC Coded Alamouti Scheme for MIMO OFDM

In the last chapter, we are aware that to achieve good error performance of a space-frequency code, we need to maximize γ, the rank of $D(C, \hat{C})$, which is determined by $\hat{\gamma}$ and LN_t, where $gam\hat{m}a$ is the column distance of the codeword difference matrix $C - \hat{C}$ and L is the number of multiple delayed paths. In the following, we investigate a space-frequency code with $N_t = 2$, which is the concatenation of a binary LDPC code , signal mapper and the Alamouti space-time code. The reason for using this concatenation is that (i) the binary LDPC code has large binary Hamming distance which can still yield a significant amount of column distance; (ii) the full rank characteristics of Alamouti space-time coding will enhance the column distance

of the concatenated coding.

3.1 LDPC Codes

Low-density parity-check (LDPC) codes were originally proposed in 1962 by Robert Gallager[18]. LDPC is a linear block codes with parity check matrices H and generator matrices G. The parity check matrix H is $N \times K$ and the generator matrix G is $(N-K) \times N$, such that $HG = 0$. Suppose that we use an $M \times N$ matrix H which has weight w_c in each column and weight w_r in each row. The constructed LDPC is call a regular LDPC, denote as a (w_c, w_r, N) code. The associated rate of this regular LDPC code is $R = 1 - w_c/w_r$. Gallager showed that the minimum distance of a regular LDPC code increases linearly with N provided that $w_c \geq 3$. The parity check matrix H needs not be regular. That means we can consider LDPC codes with varying column weights. In case of very large code lengths, there exist irregular LPDC codes with error performances superior to regular LDPC codes of similar code lengths. In most LDPC codes, N is a large number (at least several hundreds) while w_c is usually less than 10, so the density of 1s in H is quite low. That is reason for the name of low density parity check codes.

Since H is sparse, it can be represented by the lists of its nonzero locations. The mth column of H represents the mth parity check, $1 \leq m \leq M$ and the nth column of H represents the nth code bit of a codeword, $1 \leq n \leq N$. Hence, code bits can be

indexed by n (e.g. c_n) and the parity checks can be indexed by m (e.g.z_m). The set of code bits that participate in the parity check z_m (i.e. the nonzero elements in mth row of H) is denoted

$$N_m = \{n : H_{mn} = 1\}. \tag{3.1}$$

Thus we can write mth parity check as

$$z_m = \sum_{n \in N_m} c_n. \tag{3.2}$$

The set of code bits that participate in the parity check z_m except for the code bit n is denoted

$$N_{m,n} = N_m \setminus n. \tag{3.3}$$

Let $|S|$ denote the size of a set S. We see that $|N_m|$ is the number of nonzero elements in mth row of H or the number of code bits that participate in the mth parity check.

Similarly, The set of parity checks in which bit c_n participates (i.e. the nonzero elements of the nth column of H) is denoted

$$M_n = \{m : H_{mn} = 1\}. \tag{3.4}$$

For a regular LDPC code, $|M_n| = w_c$ that is the number of parity check equations

that check on the nth code bit. Let

$$M_{n,m} = M_n \setminus m. \tag{3.5}$$

be the set of parity checks in which code bit c_n participates except for check m. LDPC can be regarded as the concatenation of repeatition codes (the number of repetition is the number of checks for each code bit) and signle parity check codes (each check checks on several code bits). Then, iterative decoding between the repetition codes and single parity check codes can be implemented as follows.

3.2 Alamouti Space-Time Code

Alamouti space-time code is a simple design to transmit two orthogonal sequences respectively through the two transmit antennas in the space-time coding system with two transmit antennas. With this, full diversity, i.e., two, can be achieved, A block diagram of the Alamouti space-time coding is shown in Fig.(3.1).

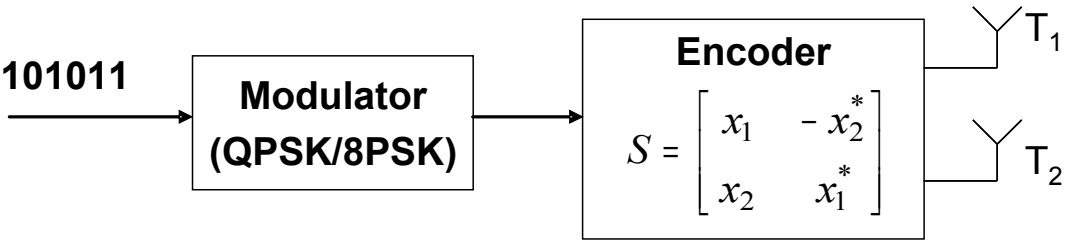

Figure 3.1: A block diagram of the Alamouti space-time encoder.

Algorithm 1 Iterative Log Likelihood Decoding Algorithm for Binary LDPC Codes

Input:

Parity check matrix $H_{M\times N}$, the maximum number of iterations L, and vector of the channel value L_c (L_c is the LLR value).

Initialization:

Set $\eta_{m,n}^{[0]} = 0$ for all (m, n) with $H(m, n) = 1$.
Set $\lambda_n^{[0]} = L_c[n]$.
Set the loop counter $l = 1$.

Check node update: For each (m, n) with $H(m, n) = 1$: Compute

$$\eta_{m,n}^{[l]} = -2\tanh^{-1}\left(\prod_{j\in N_{m,n}} \tanh(-\frac{\lambda_j^{[l-1]} - \eta_{m,j}^{[l-1]}}{2})\right) \tag{3.6}$$

Bit node update: For $m = 1, 2, \ldots, N$: Compute

$$\lambda_n^{[l]} = L_c + \sum_{m\in M_n} \eta_{m,n}^{[l]} \tag{3.7}$$

Hard Decision: Set $\hat{c}_n = 1$ if $\lambda_n^{[l]} > 0$, else set $\hat{c}_n = 0$.
If $H\hat{c} = 0$, then **Stop**.
Else if iterations$< L$, go to **Check node update**.
Else declare a decoding failure and **Stop**.

The information bits are first modulated using an 2^M-ary modulation scheme. The encoder then takes a block of two modulated symbols s_1 and s_2 as input in each encoding operation and send its output to the transmit antennas according to the code matrix[5],

$$S = \begin{bmatrix} s_1 & -s_2^* \\ s_2 & s_1^* \end{bmatrix} \tag{3.8}$$

In Eqs.(3.8), the first column represents the two symbols transmitted through the two tranmist antennas in first transmission period and the second column represents the two symbols transmitted through the two tranmist antennas in the second transmission period. The first row corresponds to the symbols transmitted through the first antenna and the second row corresponds to the symbols transmitted through the second antenna.

Consider the Alamouti scheme with two transmit antennas and two receive antennas in flat fading channel. We can rewrite Eqs.(2.2) in chapter 2.1 as

$$\begin{aligned} \begin{bmatrix} r_{11} & r_{12} \\ r_{21} & r_{22} \end{bmatrix} &= \begin{bmatrix} h_{11} & h_{12} \\ h_{21} & h_{22} \end{bmatrix} \begin{bmatrix} s_1 & -s_2^* \\ s_2 & s_1^* \end{bmatrix} + \begin{bmatrix} n_{11} & n_{12} \\ n_{21} & n_{22} \end{bmatrix} \\ &= \begin{bmatrix} h_{11}s_1 + h_{12}s_2 + n_{11} & -h_{11}s_2^* + h_{12}s_1^* + n_{12} \\ h_{21}s_1 + h_{22}s_2 + n_{21} & -h_{21}s_2^* + h_{22}s_1^* + n_{22} \end{bmatrix} \end{aligned} \tag{3.9}$$

where s_1 and s_2 are original modulation signals such as QPSK or 8PSK, and $n_{i,j}$ is

the additive complex Gaussian noise with zero mean and variance σ^2.

The receiver constructs two decision statistics based on the *linear* combination of the received signals. The decision statistics, denoted by $\widetilde{s}_1$ and $\widetilde{s}_2$, are given by

$$\begin{aligned}\widetilde{s}_1 &= h_{11}^* r_{11} + h_{12} r_{12}^* + h_{21}^* r_{21} + h_{22} r_{22}^* \\ &= \|H\|_F^2 s_1 + h_{11}^* n_{11} + h_{12} n_{12}^* + h_{21}^* n_{21} + h_{22} n_{22}^* \\ &= \|H\|_F^2 s_1 + n\end{aligned} \tag{3.10}$$

$$\begin{aligned}\widetilde{s}_2 &= h_{12}^* r_{11} - h_{11} r_{21}^* + h_{22}^* r_{12} - h_{21} r_{22}^* \\ &= \|H\|_F^2 s_2 + h_{12}^* n_{11} - h_{11} n_{21}^* + h_{22}^* n_{12} - h_{21} n_{22}^* \\ &= \|H\|_F^2 s_2 + n\end{aligned} \tag{3.11}$$

where n is the additive complex Gaussian noise with zero mean and variance $\|H\|_F^2 \sigma^2$, $\|H\|_F^2$ is the Frobenius norm of H.

From Eqs.(3.10) and Eqs.(3.11), we observe that $\widetilde{s}_1$ is only concerned about s_1 but independent of s_2. Similarly, $\widetilde{s}_2$ is only concerned about s_2 but independent of s_1. Hence we can simplify the Alamouti MIMO model to two independent system, which is shown as Fig.(3.2).

The traditional decoder of Alamouti combining is to choose a signal $\hat{s}_i$ from the

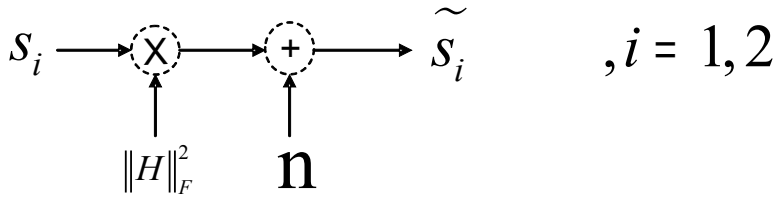

Figure 3.2: A simply model of the Alamouti space-time codes.

signal modulation constellation ϖ to minimize the Euclidean Distance

$$\begin{aligned} \hat{s}_1 &= arg \min_{\hat{s}_1 \in \varpi} d^2(\widetilde{s}_1, \hat{s}_1). \\ \hat{s}_2 &= arg \min_{\hat{s}_2 \in \varpi} d^2(\widetilde{s}_2, \hat{s}_2). \end{aligned} \tag{3.12}$$

In case that the Alamouti space-time coding is only a part of a concatenated coding system, the soft-in-soft-out (SISO) decoding of Alamouti space-time coding is desired. We can use the demapper formula for modulation as in [19]. For an arbitrary number of M modulated bits $b_{0,\cdots,M-1}$ per symbol $\widetilde{s}$ ($\widetilde{s}_1$ or $\widetilde{s}_2$) we obtain the LLR (log likelihood ratio) of *a posteriori* probability of bit b_k as

$$\begin{aligned} L(b_k \mid \widetilde{s}) &= L_a(b_k) + L_e(b_k) \\ &= L_a(b_k) \\ &+ \ln \frac{\sum_{i=0}^{2^{M-1}-1} \exp(-\frac{\|\widetilde{s} - \|H\|_F^2 \cdot map\left([(c_i)_{1:\,k-1} \quad 1 \quad (c_i)_{k:\,M-1}]\right)\|^2}{\|H\|_F^2 \, \sigma^2}) \exp(c_i L_a)}{\sum_{i=0}^{2^{M-1}-1} \exp(-\frac{\|\widetilde{s} - \|H\|_F^2 \cdot map\left([(c_i)_{1:\,k-1} \quad 0 \quad (c_i)_{k:\,M-1}]\right)\|^2}{\|H\|_F^2 \, \sigma^2}) \exp(c_i L_a)} \end{aligned} \tag{3.13}$$

where $map(\cdot)$ denotes the modulation of information bits from the signal modulation constellation ϖ, $[c_i]$ is a row vector having the values 0 or 1 according to the binary decomposition[1] of i, and $(c_i)_{a:\,b}$ denotes the part of the vector $[c_i]$ consisting of the ath element to bth element, $L_a(b_k)$ and $L_e(b_k)$ is are the LLR of the *a priori* probability of bit b_k and the extrinsic LLR value of bit b_k respectively. Using the demapper, Alamouti decoding can pass the soft value $L_e(b_k)$ instead of hard value to other decoder in the concatenated coding system for further process.

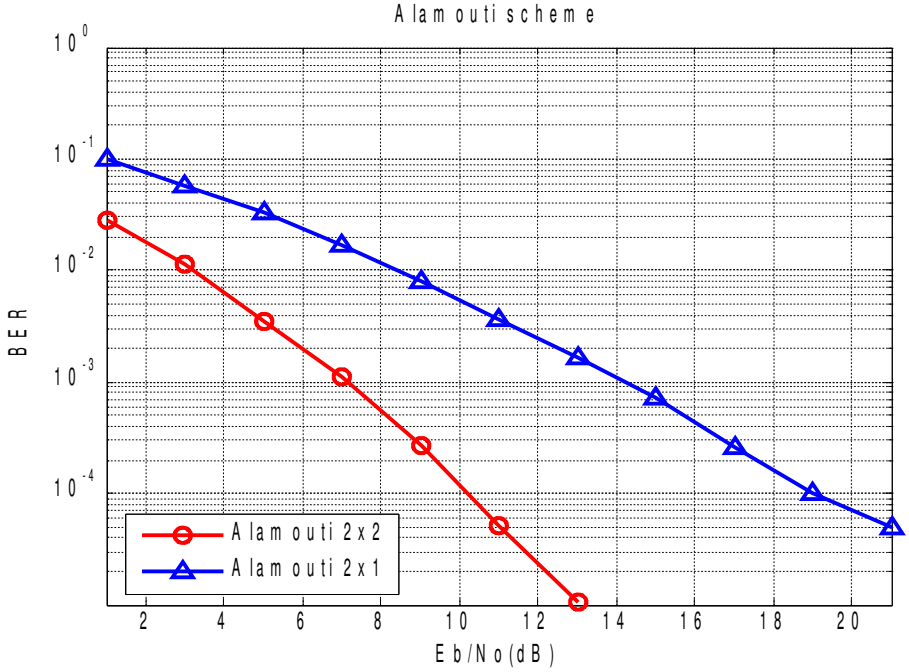

Figure 3.3: Alamouti space-time codes on flat fading channel.

Fig.(3.3) shows the bit error rate (BER) performance of Alamouti space-time code using coherent QPSK modulation.

[1]If we set $i = 21 = 1 \cdot 2^0 + 0 \cdot 2^1 + 1 \cdot 2^2 + 0 \cdot 2^3 + 1 \cdot 2^4$, the decomposition of i is a row vector $[c_i] = [c_1\ c_2\ c_3\ c_4\ c_5] = [1\ 0\ 1\ 0\ 1]$

3.3 The Space-Frequency Code Under Investigation

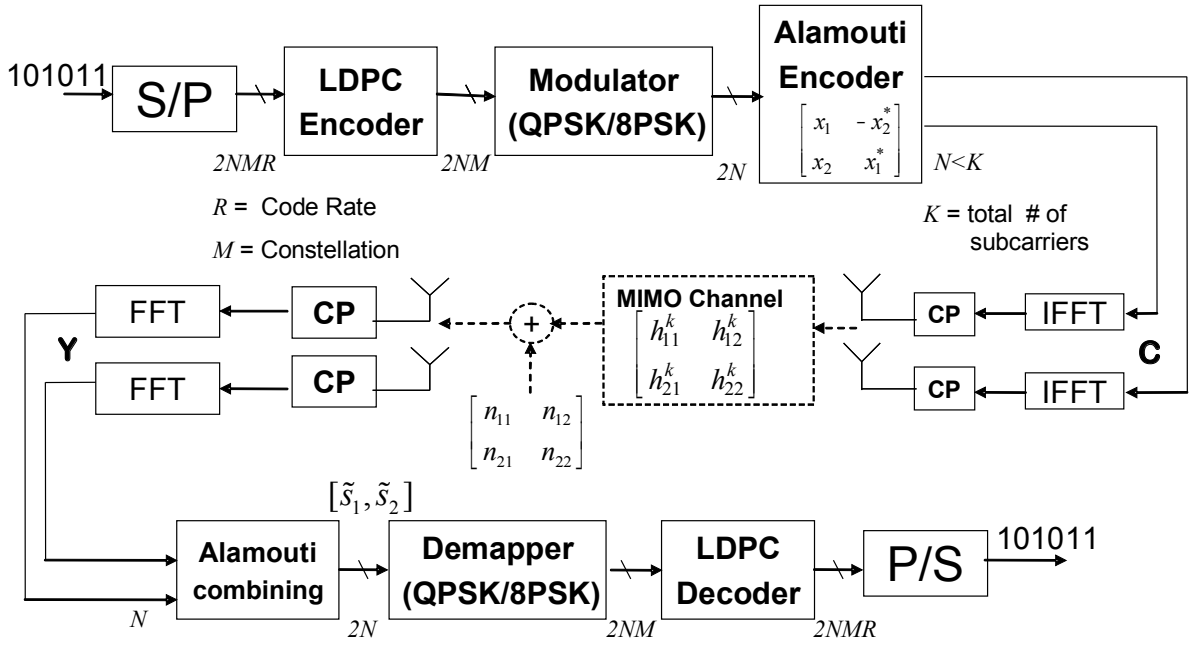

Figure 3.4: A block diagram of the space-frequency code under investigation.

By studying [20, 21, 22, 23] and Chapter 2, we believe that LDPC coded Alamouti Scheme is a good candidate to meet the design criteria shown in Chapter 2. The transmitter and receiver structure of an LDPC coded Alamouti Scheme for MIMO OFDM systems is illustrated in Fig.(3.4). We assume that the receiver has perfect channel state information (CSI).

In Fig.(3.4), the $2NMR$ information bits are first encoded by a rate R LDPC encoder into $2NM$ coded bits and then the binary LDPC coded bits are modulated

into $2N$ 2^MPSK [2] symbols. We split these $2N$ symbols into 2 streams, and each stream has N symbols. The N symbols of each stream are transmitted from one transmit antenna which has K subcarrier over an OFDM slot. Usually, we set $N < K$ in order to reserve subcarriers for side information (SI) or some other purposes. We have two streams denoted C_a and C_b which will be transmitted trough two transmit antennas respectively. The Alamouti encoder converts these two streams into a space frequency codeword represented by $[C_1, C_2]$, where C_1 and C_2 are described as

$$C_1 = \begin{bmatrix} C_a \\ C_b \end{bmatrix} = \left[\begin{array}{cccc|ccc} c_1(0) & \dots & c_1(N-1) & c_1(N) & c_1(N+1) & \dots & c_1(K) \\ c_2(0) & \dots & c_2(N-1) & c_2(N) & c_2(N+1) & \dots & c_2(K) \end{array}\right] \quad (3.14)$$

$$C_2 = \begin{bmatrix} -C_b^* \\ C_1^* \end{bmatrix} = \left[\begin{array}{cccc|ccc} -c_2^*(0) & \dots & -c_2^*(N-1) & -c_2^*(N) & -c_2^*(N+1) & \dots & -c_2^*(K) \\ c_1^*(0) & \dots & c_1^*(N-1) & c_1^*(N) & c_1^*(N+1) & \dots & c_1^*(K) \end{array}\right] \quad (3.15)$$

each $c_i(j)$ is an 2^MPSK symbol, and $c_1(N+1) = \ldots = c_1(K) = c_2(N+1) = \ldots = c_2(K) = 0$. The symbols represented by C_1 is transmitted in the first OFDM time slot and the symbols represented C_2 is transmitted in the following OFDM time slot. The transmitter applies an K-point IFFT to each row of the matrix C_i and then appends a cyclic prefix (CP), which is then used for transmission.

It is assumed that the fading process remains static during two consecutive OFDM time slots and the fading at every two consecutive OFDM time slots is independent

[2] For example, $M = 2$ for QPSK, $M = 3$ for 8PSK.

of any other two consecutive OFDM time slots.

At the receiver, we have receives signals from two receive antennas. After matched filtering and sampling, the FFT is applied to the discrete-time signal to obtain

$$\begin{aligned} Y_1 &= \begin{bmatrix} y_1^1(0) & y_1^1(1) & \dots & y_1^1(K) \\ y_2^1(0) & y_2^1(1) & \dots & y_2^1(K) \end{bmatrix} \\ Y_2 &= \begin{bmatrix} y_1^2(0) & y_1^2(1) & \dots & y_1^2(K) \\ y_2^2(0) & y_2^2(1) & \dots & y_2^2(K) \end{bmatrix} \end{aligned} \tag{3.16}$$

where y_k^i denotes the received signal at the kth subcarriers for ith OFDM time slot, $i = 1, 2$, and y_k^i can be obtained from Eqs.(2.8). The decoding consists two stages, i.e., the *soft* Alamouti combing and the *soft* LDPC decoder and the so-called extrinsic information passed from first stage to second.

For the first stage of Alamouti combing, Alamouti decoder takes $y_1^1(k)$, $y_2^1(k)$, $y_1^2(k)$ and $y_2^2(k)$ to a matrix as in Eqs.(3.9), which can be written as

$$\begin{bmatrix} r_{11} & r_{12} \\ r_{21} & r_{22} \end{bmatrix} = \begin{bmatrix} y_1^1(k) & y_1^2(k) \\ y_2^1(k) & y_2^2(k) \end{bmatrix} \tag{3.17}$$

and Alamouti soft decoding can be obtained from equations as Eqs.(3.10), Eqs.(3.11) and Eqs.(3.13) for $k = 0, 1, \dots, N-1$. For each k, there is a pair of symbols $(\widetilde{s}_1, \widetilde{s}_2)$. For s_1 and s_2, there are both M associated LLR values obtained by Eqs.(3.13), Each

LLR value corresponds to an LDPC coded bit. A total of $2NM$ LLR values are used as the vector L_c in Algorithm 1. After LDPC decoding by using Algorithm 1, we obtain $2NM$ hard value (1 or 0) for coded bits. Then, $2NMR$ information bits are detected. The LDPC decoding can produce soft output, which can be fed back to the demapper of Alamouti coding for outer iterations (other than the inner iterations inside the LDPC decoding operation). Simulation shows that such outer iterations will be significantly reduce the BER. Hence, in the rest of this report, we only consider the decoding without outer iterations.

3.4 Simulation Results

In this section, we provide computer simulation results to examine the performance of the LDPC-coded Alamouti scheme. The characteristics of the fading channels are described in Section 2.2.1. In the following simulations, the available bandwidth is 1MHz and the number of subcarriers is $K = 256$. Thus, the OFDM word duration is $T = 256\mu s$ without the cyclic prefix. We set the length of cyclic prefix to $5\mu s$ to combat the effect of inter-symbol-interference, since the delay is no more than $5\mu s$.

We simulated the space frequency codes with different power delay profiles: (i) a two-ray equal power delay profile and (ii) COST207[24] typical urban six-ray power delay profile. The subcarrier path gains are generated according to Eqs.(2.9), independently for different transmit and receive antennas. The power delay profile of the

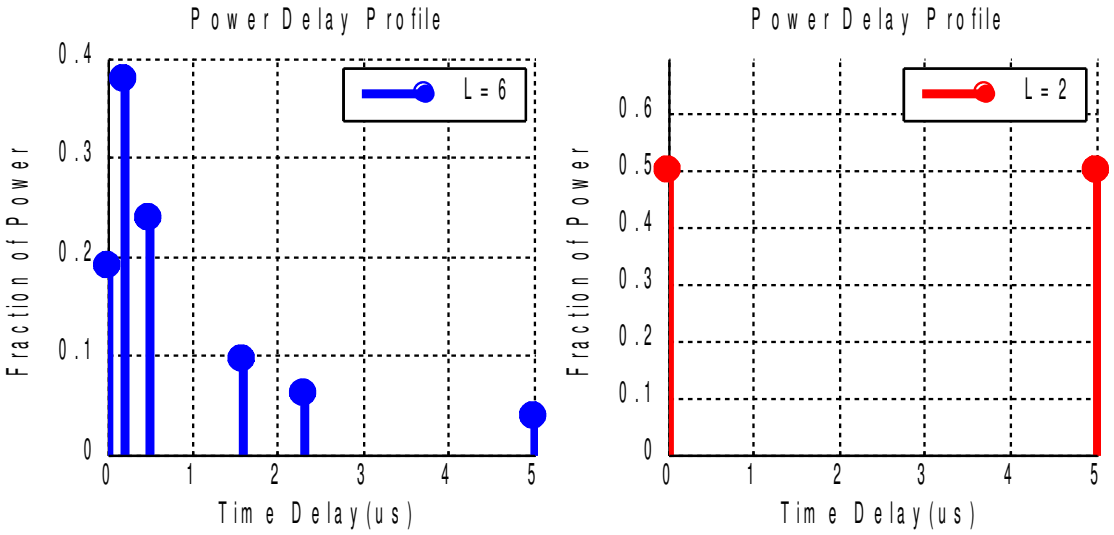

Figure 3.5: Power delay profile of six paths and two paths.

channel is shown in Fig.(3.5) and Table(3.1). All the LDPC codes used in simulation

Six paths			Two paths		
Delay (us)	Fractional Power	Doppler Category	Delay (us)	Fractional Power	Doppler Category
0.0	0.189	CLASS	0.0	0.500	CLASS
0.2	0.379	CLASS	5.0	0.500	CLASS
0.5	0.239	CLASS			
1.6	0.095	GAUS1			
2.3	0.061	GAUS1			
5.0	0.037	GAUS1			

Table 3.1: Numeric power delay profile of six paths and two paths.

are regular LDPC codes with column weight $w_c = 3$ in the parity-check matrix and with appropriate block lengths and code rates. The modulation under consideration are QPSK or 8PSK constellation respectively. Simulation results are shown in terms of the information bit-error rate (BER) versus E_b/N_0. The simulation MIMO system has $K = 256$ subcarriers. The LDPC has code rate $R = 0.5$ and the iterations of

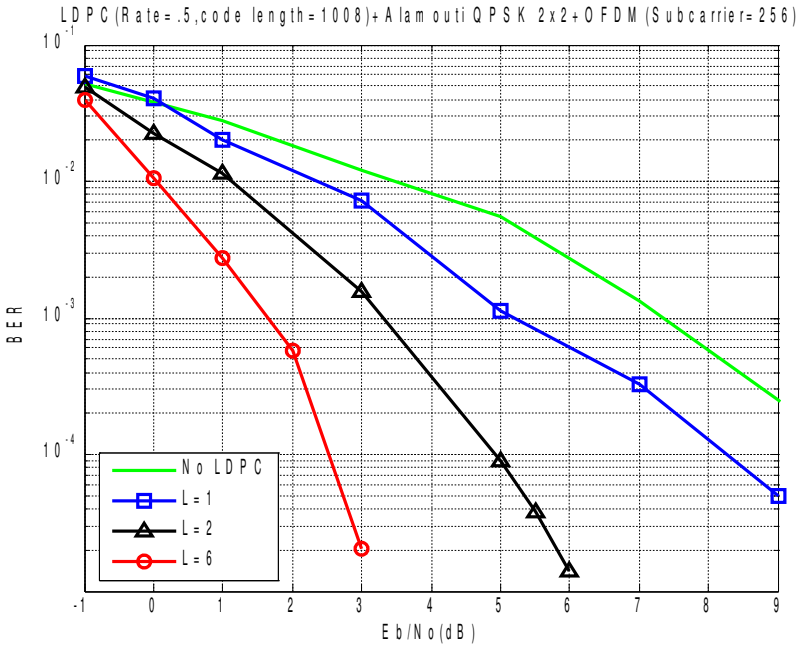

Figure 3.6: BER of considered SF codes, $N_t = N_r = 2$, QPSK modulation

LDPC codes is 30.

In order to span LDPC coded bits in an OFDM word, the LDPC code length varies with modulation. That is, the LDPC code lengths are 1008 and 1512 with respect to QPSK and 8PSK respectively. Both cases have the same number of modulation symbols, which is $1008/2 = 1512/3 = 504$. The 504 symbols are transmitted by two transmit antennas. Hence, there are 252 modulated symbols to be transmitted by each antenna. Thus, 252 of the 256 subcarriers will be used to represent the 252 symbols, while 4 of the 256 subcarriers are free subcarriers which can be used to carry side information or some other purpose. When the LDPC decoder receive (Y_1, Y_2), an LDPC codeword can be completely decoded.

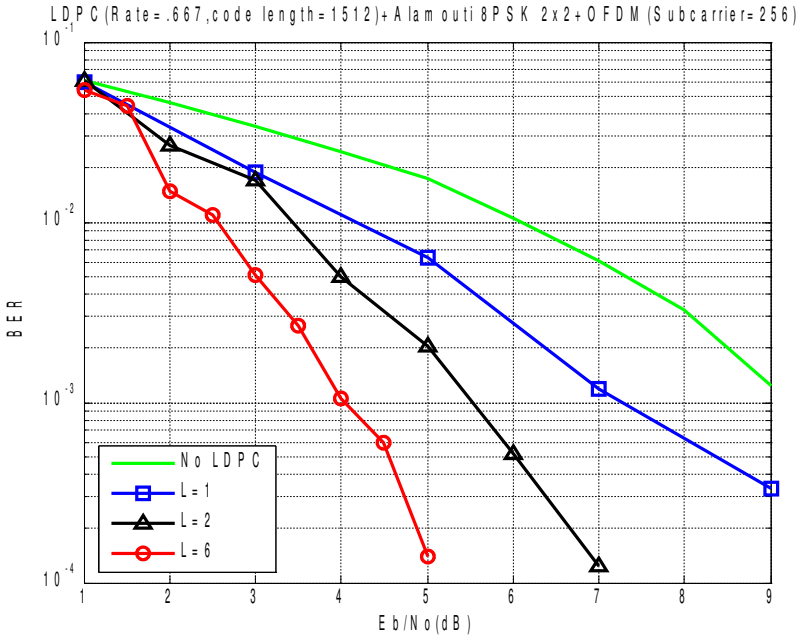

Figure 3.7: BER of considered SF codes, $N_t = N_r = 2$, 8PSK modulation

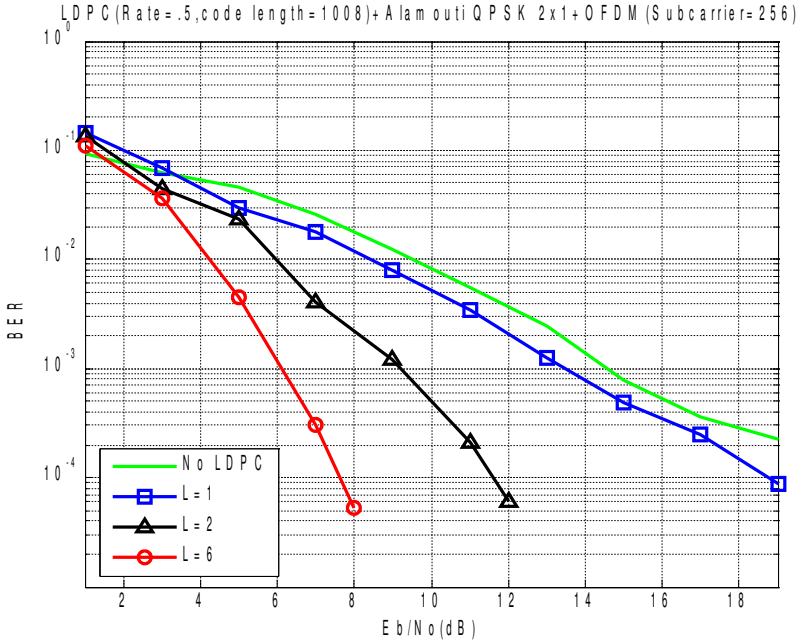

Figure 3.8: BER of considered SF codes, $N_t = 2, N_r = 1$, QPSK modulation

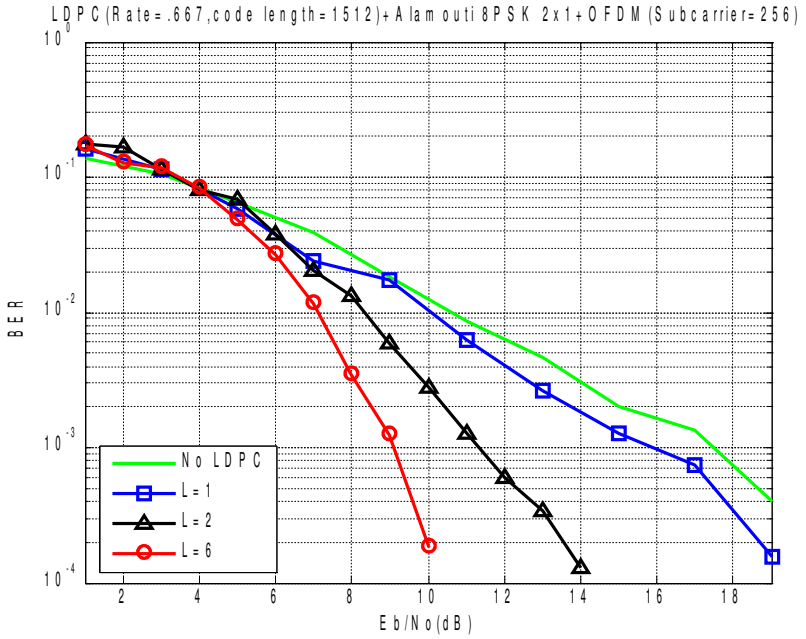

Figure 3.9: BER of considered SF codes, $N_t = N_r = 1$, 8PSK modulation

Fig.(3.6), Fig.(3.7), Fig.(3.8) and Fig.(3.9) depict the performances of the considered space-frequency (SF) codes under the condition of various power delay profiles and various modulation methods. We use the BPSK modulation for the case of not using LDPC and QPSK for the case of using LDPC codes in Fig.(3.6) and Fig.(3.8). Also, we use the QPSK modulation for the case of not using LDPC and 8PSK for the case of using LDPC codes in Fig.(3.7) and Fig.(3.9). Thus, the transmission rate of both cases are the same. Clearly, the performance of the SF codes *without* LDPC[3] codes, i.e., pure Alamouti coding is much worse than the case of using LDPC codes.

[3]The performance of the case without LDPC is independent of the condition of the existence or nonexistence of delay paths.

Chapter 4

PAPR Reduction in MIMO OFDM Systems

In OFDM systems, peak-to-average power ratio (PAPR) is an important issue for the transmitter because a system with a large PAPR requires the linear power amplifier with a large dynamic range. The problem of PAPR is due to the fact that in OFDM systems, the summation of various signals of many subcarriers will lead to the probable occurrence of high peak power as compared to the average power. For MIMO OFDM, the problem of PAPR is similar to the conventional OFDM system. The techniques used for mitigating the PAPR effect in the conventional OFDM system can also be applied to the MIMO OFDM systems. However, the usage of multiple transmit antennas may somewhat deepen the problem of PAPR while the usage of

multiple transmit antennas may provide additional room for executing the operation of PAPR reduction.

By now, many techniques have been proposed for relieving the PAPR problem in the OFDM systems, such as Amplitude Clipping, Coding, Selective Mapping (SLM) [11, 12] and Active Constellation Extension (ACE) [13]. In particular, there is a technique, called the "cross-antenna rotation and inversion"[14] (CARI) which addresses on PAPR reduction for the MIMO-OFDM systems. Our research team has recently devised a there time-shifted PAPR reduction technique for the ordinary OFDM system that is a modified form of selective mapping technique which has the advantage of low complexity and will appear in [25]. We find that after some modification, the technique is very suitable for the MIMO-OFDM system. We call this new PAPR reduction technique for MIMO-OFDM systems "Time-domain circular shift (TDCS)" technique. We will compare the cross-antenna rotation and inversion[14] (CARI) with TDCS. The numeric result will show the advantage of TDCS in Chapter 4.4.

4.1 Basics of PAPR

After the IFFT operation, the resulting complex baseband OFDM signal is

$$s(t) = \frac{1}{\sqrt{K}} \sum_{k=0}^{K-1} X_k \exp^{j2\pi kt/K}, \quad 0 \le t \le T \tag{4.1}$$

where T is the duration of an OFDM symbol and X_k is the data symbol considered in the frequency domain. The PAPR of this OFDM system can be defined as 1.

DEFINITION 1 *For any baseband OFDM signal, the PAPR of the OFDM symbol can be expressed as*

$$\mathrm{P}APR = \frac{\max_{0\leq t<T} |s(t)|^2}{E\{\, |s(t)|^2\}}. \tag{4.2}$$

where $E\{x\}$ denotes the expectation function of x.

In case of the discrete-time OFDM system, enough oversampling on the OFDM symbol is required to preserve the accurate PAPR value [26]. Suppose that oversampling factor is J. The discrete-time OFDM signal can be written as

$$s_n = \frac{1}{\sqrt{K}} \sum_{k=0}^{K-1} X_k \exp^{j2\pi kn/JK}, \quad n = 0, \cdots, JK-1. \tag{4.3}$$

Thus, the PAPR of the discrete-time OFDM signal is shown in Definition 2.

DEFINITION 2 *The PAPR of the OFDM symbol in discrete-time signals is*

$$\mathrm{P}APR = \frac{\max_{0\leq n<JK} |s_n|^2}{\frac{1}{JK}\sum_{n=0}^{JK-1} |s_n|^2}. \tag{4.4}$$

The case of $J = 1$ is called Nyquist rate sampling or critical sampling. The case of $J > 1$ is called oversampling. For $J = 4$, the peak of continuous-time value can be estimated sufficiently.

The complementary cumulative distribution function (CCDF) of the PAPR can be used to evaluate the capability of PAPR reduction. Here, CCDF is defined as the probability of the occurrence of PAPR exceeding a given threshold $PAPR_0$, which is

$$CCDF = P_r(PAPR > PAPR_0). \tag{4.5}$$

Consider MIMO OFDM systems with N_t transmit antennas and N_r receive antennas. Denote $PAPR_p$ as the PAPR of the pth transmit antenna. Then for multiple transmit antennas, the PAPR is defined in Definition 3.

DEFINITION 3 *The PAPR of the MIMO OFDM symbol in discrete-time signals is as below*

$$\overline{\mathrm{P}APR} = max(PAPR_1, PAPR_2, \ldots, PAPR_{N_t}). \tag{4.6}$$

$$\mathrm{P}APR_p = \frac{\max_{0 \le n < JK} |s_n^p|^2}{\frac{1}{JK}\sum_{n=0}^{JK-1} |s_n^p|^2}, \quad p = 1, 2, \ldots, N_t. \tag{4.7}$$

where N_t is transmit antenna, $PAPR_p$ is the PAPR of transmit antenna p, and s_n^p is the discrete OFDM signal of transmit antenna p.

In case that selective mapping technique is used for PAPR reduction. We assume that the number of candidates for the selective mapping operation scheme is Q. The selector choose the candidate with the lowest $\overline{PAPR}$. In other words, a minimax

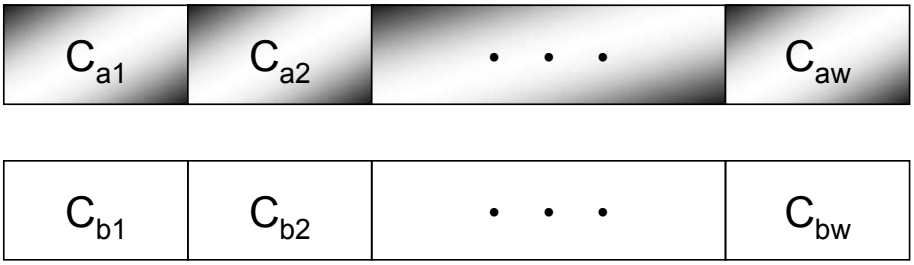

Figure 4.1: Partition of the C_a and C_b.

criterion is used, which can be described as

$$(\underline{s}_1, \ldots, \underline{s}_{N_t}) = \arg \min_{s_1, \ldots, s_{N_t}} (\overline{PAPR}) \tag{4.8}$$

where $(\underline{s}_1, \ldots, \underline{s}_{N_t})$ are transmitted OFDM symbols with lowest PAPR, and by Eqs.(4.7) $s_p = (s_{p,0}, \ldots, s_{p,JK})$ which is time-domain signal for transmit antenna p.

4.2 CARI Scheme

We now describe the CARI scheme[14] with $N_t = 2$ based on the MIMO OFDM investigated in Section (3.3). We consider the space-frequency code described by Eqs.(3.14) and Eqs.(3.15). It is easy to show that C_i and $\pm C_i^*(i = a, b)$ have the same PAPR properties. Therefore, for the LDPC coded Alamouti scheme, the PAPR reduction needs to be done only for C_1 in Eqs.(3.14).

For CARI, we partition the C_a and C_b into W subblocks of equal sizes, denoted

as

$$C_a = \begin{bmatrix} C_{a1} & C_{a2} & \cdots & C_{aW} \end{bmatrix} \tag{4.9}$$

$$C_b = \begin{bmatrix} C_{b1} & C_{b2} & \cdots & C_{bW} \end{bmatrix} \tag{4.10}$$

Each subblock has K/W elements in it as shown in Fig.(4.1). Now we perform anti-clockwise rotation and inversion across 2 antennas, which is shown in Fig.(4.2) and Table(4.1). That is, there are four kinds of candidates for each pair of C_{ai} and C_{bi}. With W subblocks and 2 antennas, 4^W candidates can be obtained. In case that

	Operation $(i = 0, 1, \ldots, W)$
I	C_{ai} and C_{bi} are unchanged
II	C_{ai} and C_{bi} are swapped
III	C_{ai} and C_{bi} are inverted, i.e.,$-C_{ai}$ and $-C_{bi}$
IV	C_{ai} and C_{bi} are swapped and inverted, i.e., $-C_{ai}$ and $-C_{bi}$ are swapped

Table 4.1: Four operations of each subblock.

M is large, this method will be impractical, since we have to search a large number of candidates to obtain the best PAPR. Hence, a suboptimal method is considered in [14], which is called Successive Suboptimal CARI (SS-CARI) scheme. The block diagram is shown in Fig.(4.3). At the beginning, the operations for C_{a1} and C_{b1} in Table(4.1) are executed. Then, PAPR values of the four candidates are calculated. For example, if the operation II has the lowest PAPR, the fist subblock is fixed as shown in 4.4. Next, four operations for C_{a2} and C_{b2} are performed and the PAPR

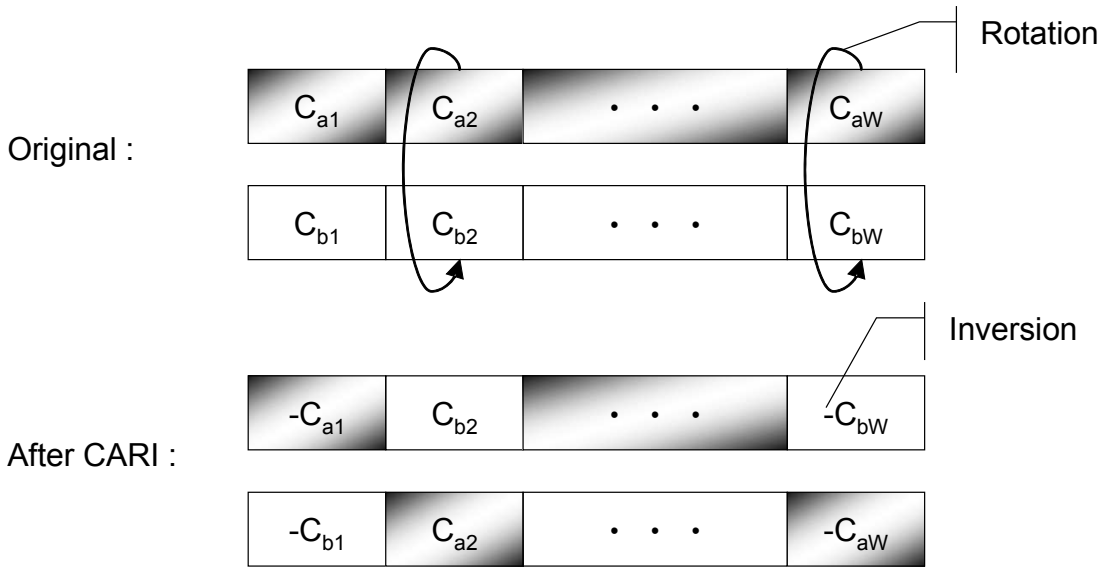

Figure 4.2: Cross-Antenna Rotation and Inversion (CARI) scheme.

values of the four candidates are calculated. Again, the second subblock is fixed with the lowest PAPR. By proceeding this to all W subblocks, a total of $4W$ candidates can be obtained which is less than 4^W candidates in CARI scheme. Note that $S = 2W$ bits for side information are still needed for the SS-CARI.

In Section (4.3), we will propose a novel method to reduce the PAPR of MIMO-OFDM in time domain. To compare to the proposed time-domain scheme, we set the partition number to be $W = Q/4$ for SS-CARI, where $Q = 8, 16, \ldots$ is the total number of candidates. In Fig.(4.3), we observe that the transmitter needs $2Q$ IFFT computations in order to obtain Q candidates. The proposed method described in Section (4.3) will need only two IFFT computations.

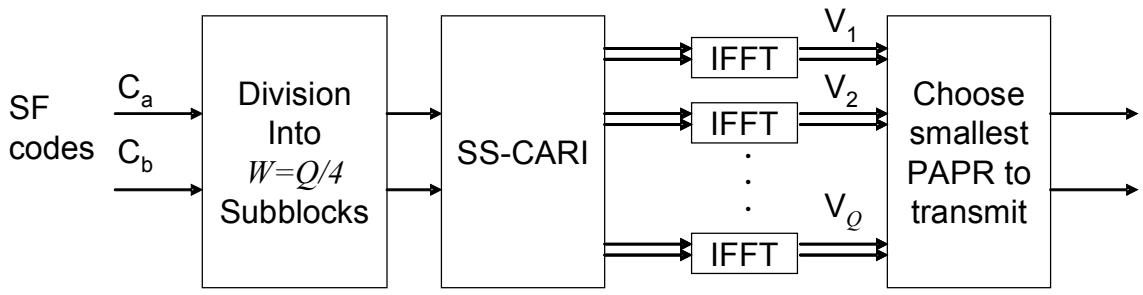

Figure 4.3: Block diagram of SS-CARI scheme.

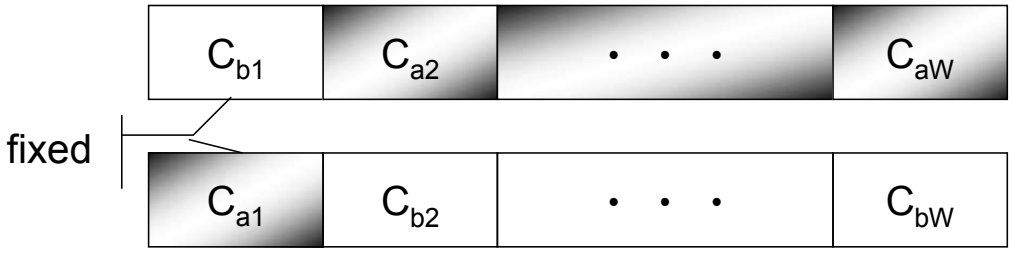

Figure 4.4: Successive Suboptimal Cross-Antenna Rotation and Inversion (SS-CARI) scheme.

4.3 Time-Domain Circular Shift Scheme

Now we will show our main result of this research that is Time-Domain Circular Shift Scheme (TDCS) for PAPR reduction in the MIMO-OFDM system.

4.3.1 Time-Domain Circular Shift Scheme

The time-domain circular shift (TDCS), which produces candidates in time-domain instead of in frequency domain, is depicted in Fig.(4.5). The time-domain OFDM

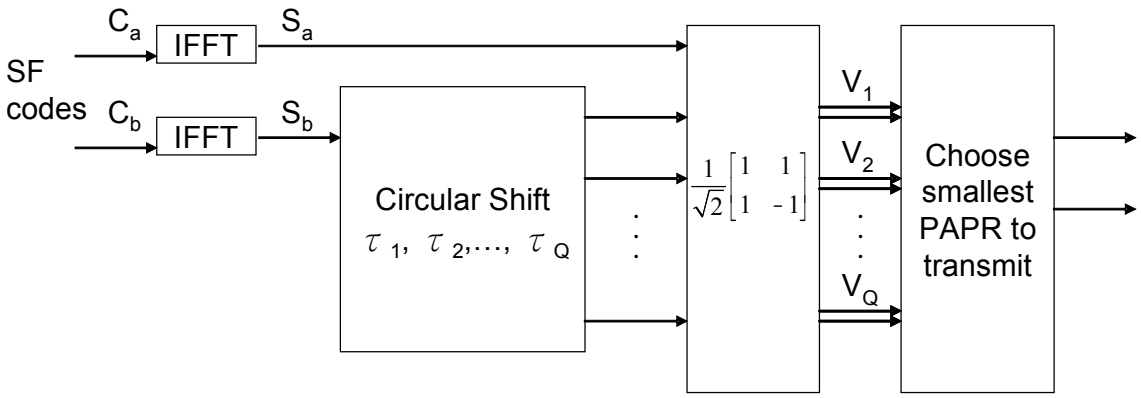

Figure 4.5: Time-domain circular shift (TDCS) scheme.

symbols for two transmit antennas are denoted as

$$S_a = \begin{bmatrix} S_{a1} & S_{a2} & \cdots & S_{a,\,JK} \end{bmatrix} \tag{4.11}$$

$$S_b = \begin{bmatrix} S_{b1} & S_{b2} & \cdots & S_{b,\,JK} \end{bmatrix} \tag{4.12}$$

We apply a circular shift[1] with parameter τ_i on S_b $(i = 1, \ldots, Q)$. We denote the circular-shifted signals for parameter τ_i by $\widehat{S}_b^{\,i}$, where

$$\widehat{S}_b^{\,i} = \begin{bmatrix} \widehat{S}_{b1}^{\,i} & \widehat{S}_{b2}^{\,i} & \cdots & \widehat{S}_{b,\,JK}^{\,i} \end{bmatrix} \tag{4.13}$$

Then, we multiply the combination of S_a and $\widehat{S}_b^{\,i}$ by a unitary matrix U to obtain a

[1] A circular shift is a permutation of the entries in a tuple where the last element becomes the first element and all the other elements are shifted, or where the first element becomes the last element and all the other are shifted.

candidate for parameter τ_i. The ith candidate will be

$$V_i = \begin{bmatrix} V_a^i \\ \\ V_b^i \end{bmatrix} = U \begin{bmatrix} S_{a1} & S_{a2} & \cdots & S_{a,\,JK} \\ \\ \widehat{S}_{b1}^{\,i} & \widehat{S}_{b2}^{\,i} & \cdots & \widehat{S}_{b,\,JK}^{\,i} \end{bmatrix} \tag{4.14}$$

where V_a^i and V_b^i are the OFDM symbols for the first and the second transmit antennas respectively and,

$$U = \frac{1}{\sqrt{2}} \begin{bmatrix} 1 & 1 \\ \\ 1 & -1 \end{bmatrix} \tag{4.15}$$

We have one candidate for each shift. Hence there are Q candidates in total. We use minimax criterion to find the lowest PAPR and transmitted OFDM symbols according to Eqs.(4.6) and Eqs.(4.8).

From Fig.(4.5) we observe that only *two* IFFT computations are needed and the number of bits for side information is $S = \log_2 Q$. Thus, TDCS can reduce the implementation complexity as compared to SS-CARI and is more applicable to practical systems.

4.4 Simulation Results

In this section, we provide the simulation results so that we can compare the performances of SS-CARI and the proposed TDCS regarding CCDF and BER (bit error rates).

4.4.1 CCDF Performance

In our simulation, 10^5 random OFDM sequences are generated to obtain the CCDF. We use $N_t = 2$ and $K = 128$ subcarriers. The modulation is QPSK. Oversampling factor J is set to 4..

	$Q = 8$		$Q = 16$	
PAPR Scheme	Side Information S bits	IFFT Number ξ	Side Information S bits	IFFT Number ξ
TDCS	3	2	4	2
SS-CARI	4	16	8	32

Table 4.2: Comparison of information bit S and the number of IFFT needed ξ.

Fig.(4.6) shows the CCDF of PAPR for the TDCS and SS-CARI scheme using $Q = 8$ and $Q = 16$ candidates respectively. The proposed TDCS scheme for $Q = 8$ achieves better performance than the SS-CARI scheme for $W = 2$. The TDCS and SS-CARI schemes for $Q = 16$ perform almost the same. We list the number of needed side information bits and the number of needed IFFT computations for both TDCS and SS-CARI in Table(4.2). We can observe that both the side information S and the number of IFFT computations needed ξ for TDCS scheme are less than that for SS-CARI scheme.

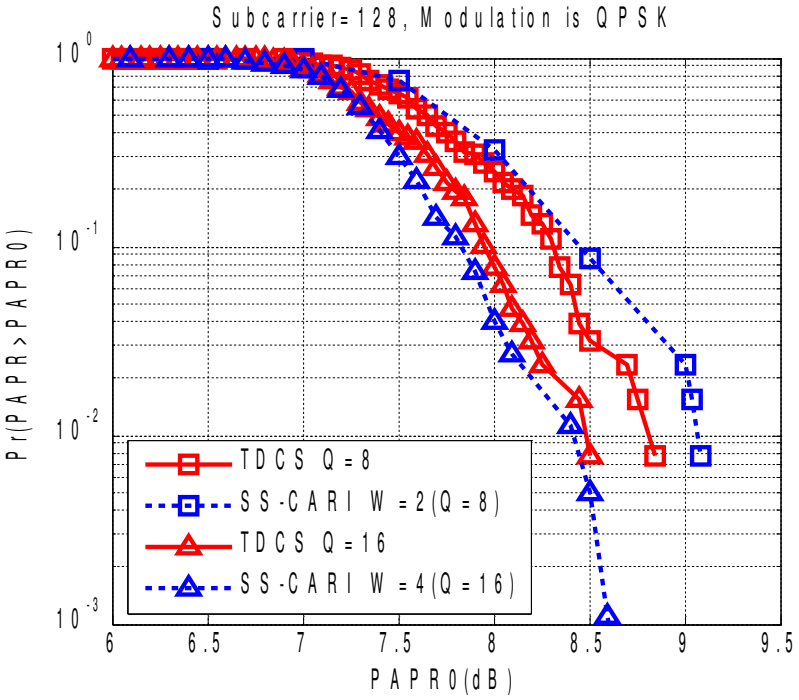

Figure 4.6: SS-CARI and TDCS scheme for different value of candidates Q.

4.4.2 BER Performance

In many PAPR research works, the effect on BER is neglected. In fact, the effect on BER may be great in some cases. In our simulation, we use $N_t = 2$ and $K = 256$ subcarriers. The available bandwidth is 1MHz and the subcarrier $K = 256$. We consider the channel with power delay profiles: COST207[24] typical urban six-ray power delay profile. The subcarrier path gains are generated according to Eqs.(2.9), independently for different transmit and receive antennas. The oversampling factor is $J = 4$. All the other parameters are just the same as what we use in Section (3.4).

Fig.(4.7) and Fig.(4.8) show the performance of SS-CARI and TDCS using the

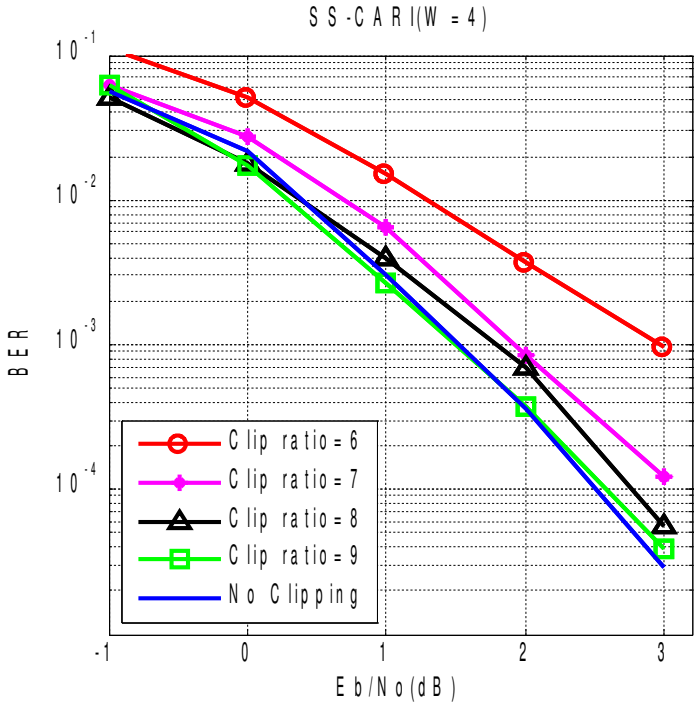

Figure 4.7: SS-CARI BER performance for $W = 4$.

space frequency code investigated in Section (3.3). In the simulation, we assume that CSI and side information can be recovered correctly by the receiver. Take 7dB clipping ratio case as example. We can observe that the BER performance of both schemes are around 10^{-4} at $E_b/N_0 = 3$dB.

In Eqs.(4.14), multiplying unitary matrix U to the left side of a space-frequency codeoword will not effect the BER performance. Hence the U can be designed by any unitary matrix other than that shown in Eqs.(4.15)

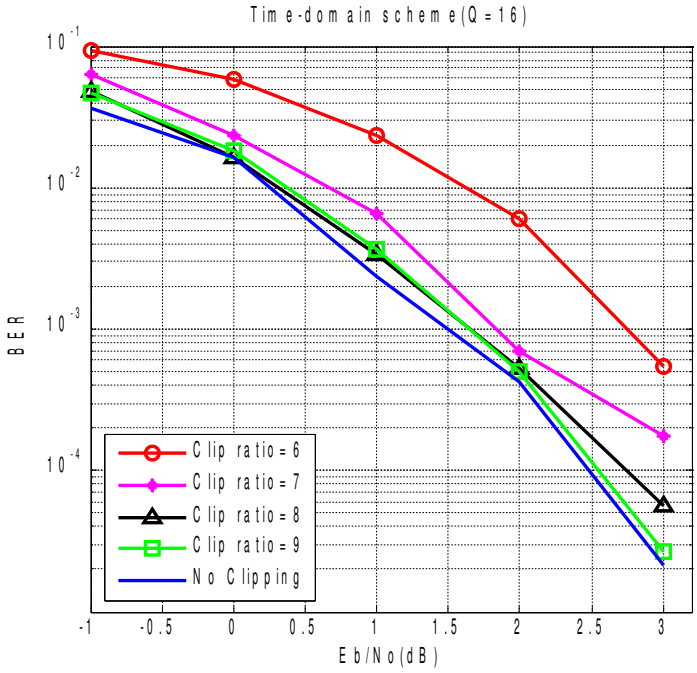

Figure 4.8: TDCS BER performance for $Q = 16$.

Side Information Embedded

In some situations, the side information is embedded into the system. There are many methods to embed the side information into the system. A major concern is that the side information must be well protected. Otherwise, serious error propagation will occur. Here, we consider a simple method which is obtained by inserting the side information into the zero terms of Eqs.(3.14) and Eqs.(3.15) and each reserved subcarrier contains one side information bit. In fact, we can insert more than one bit to one subcarrier if the system needs a large number of the side information bits. In order to protect the side information bit, the power of side information signals is transmitted four times of original signals. The performance of SS-CARI scheme

remain similar to TDCS scheme, shown in Fig.(4.9) and Fig.(4.10). Take the 7dB clipping ratio condition as example, we can observe that the BER performance of both schemes are around 10^{-4} at $E_b/N_0 = 3$dB. That is, the system suffers no BER performance degradation by inserting the side information bits in the simple methods described above.

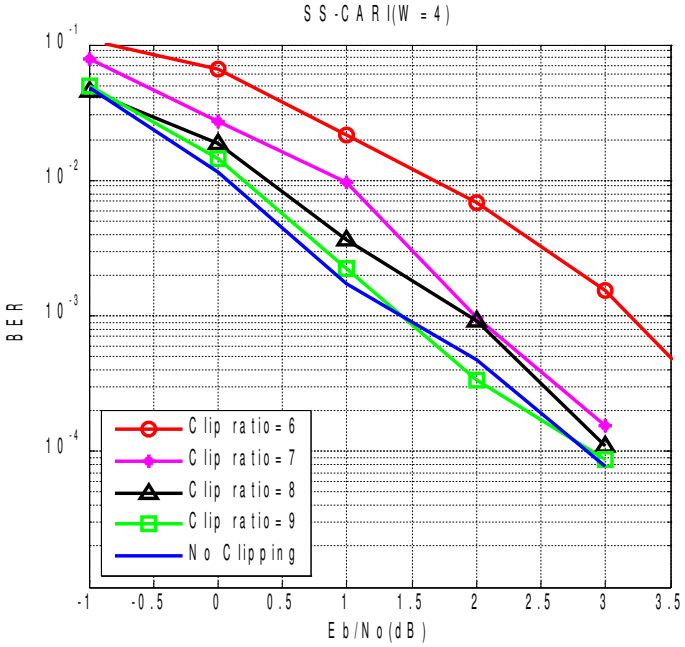

Figure 4.9: SS-CARI BER performance for $W = 4$ with side information embedded.

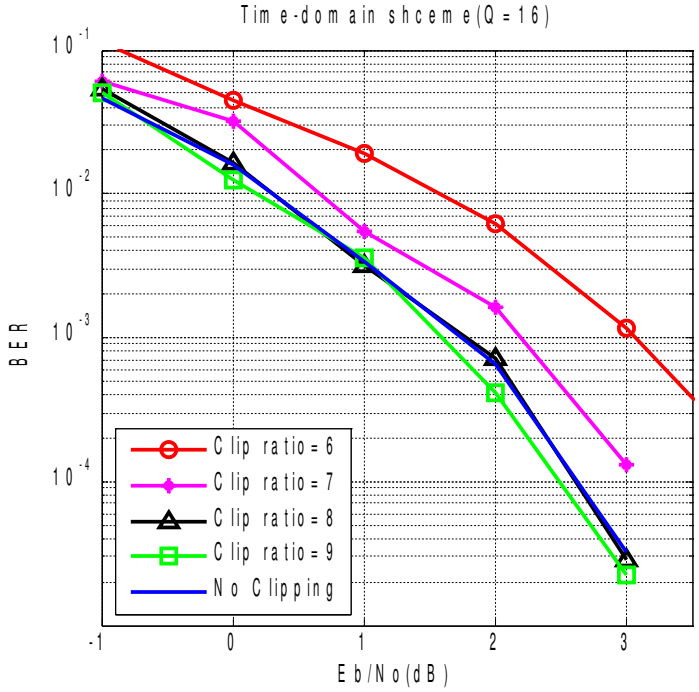

Figure 4.10: TDCS BER performance for $Q = 16$ with side information embedded.

Chapter 5

CONCLUSIONS AND SELF EVALUATION

In this three-year project, our goal is to investigate MIMO-OFDM systems so that both low PAPR and error rates can be achieved. In the first year, we investigate a space-frequency code with two transmit antennas that is constructed by the concatenation of binary LDPC code and the Alamouti space-time coding. The reason for choosing such a design is that this construction can achieve large column distance and full rank of the codeword difference matrix, which will ensure large diversity for combating the multi-path fading MIMO-OFDM channel. Simulation results verify that the construct space-frequency code does perform well in the MIMO-OFDM channel. Based on this efficient space-frequency code, we propose a low complexity

selective-mapping type PAPR reduction technique. In the proposed technique, the candidates are generated in the time-domain instead of the frequency domain. Thus, only two IFFT operations are needed in the proposed technique while for the selective mapping using frequency domain many IFFT operations are needed. In case the number of candidates is not great (no more than 16), the proposed technique can significantly reduce the complexity without sacrificing the PAPR reduction capability and error rates. Simulation results verify the advantage of the proposed PAPR reduction technique.

Some of the results of this research comes from the PhD thesis of S.K. Deng [25] and the master thesis of Y. H. Lo [27]

As a summary, we have a very significant research result in this first-year term, i.e., the time-domain PAPR reduction technique for the MIMO-OFDM system. The idea is novel and the advantage is obvious in case the number of selective mapping is not large. We believe that this result can be published in prestigious academic conferences and journals.

Bibliography

[1] H. Jafarkhani V. Tarokh and A. R. Calderbank. "Space-time block codes from orthogonal designs". *Information Theory, IEEE Transactions on*, pages pp. 1456–1467, Jul. 1999.

[2] N. Seshadri V. Tarokh and A. R. Calderbank. "Space-time codes for high data rate wireless communication: Performance criteria and code construction". *IEEE Trans. Inform. Theory*, pages 744–764, Mar. 1998.

[3] G. Bauch S. Baro and A. Hansmann. "Improved codes for space-time trellis-coded modulation". *Communications Letters, IEEE*, pages pp. 20–22, Jan. 2000.

[4] G. J.Foschini Jr. "Layered space-time architecture for wireless communication in a fading environment when using multi-element antennas". *Bell Labs Tech. J.*, pages pp. 41–59, 1996.

[5] S.M. Alamouti. "A simple transmit diversity technique for wireless communications". *IEEE Journal on Selected Areas in Communications*, 16(8):pp. 1451–1458, Oct 1998.

[6] Chiu W.H. and Su H.J. "New Optimal Rate-Diversity Tradeoff Space-Time Codes with Adaptive Iterative Decoding". *ISITA*, Oct 2006.

[7] G.Yi and K. B.Letaief. "Performance Evaluation and Analysis of Space-time Coding in Unequalized Multipath Fading Links". *IEEE Trans. Commun.*, Nov. 2000.

[8] L. J.Cimini Jr. "Analysis and simulation of a digital mobile channel using orthogonal frequency division multiplexing". *IEEE Trans. Commun.*, pages pp. 665–675, Jul. 1995.

[9] A.J. Bolcskei, H. Paulraj. "Space-frequency coded broadband OFDM systems". *in Proc. 48th IEEE Vehicular Technology Conf.*, 1:pp. 1–6, Sep. 2000.

[10] A. Naguib D. Agarwal, V. Tarokh and N. Seshadri. "Space-time coded OFDM for high data rate wireless communication over wideband channels". *in Proc. 48th IEEE Vehicular Technology Conf.*, pages 2232–2236, May 1998.

[11] R. Fischer R. Bauml and J. Huber. "Reducing the peak-to-average power ratio of multicarrier modulation by selected mapping,". *Electronic Letters*, pages pp. 2056–2057, 1996.

[12] G. Wade J. V. Eetvelt and M. Tomlinson. "Peak to average power reduction for OFDM schemes by selective scrambling,". *Electronic Letters*, pages pp. 1963–1964, 1996.

[13] B. Krongold and D. Jones. "PAR reduction in OFDM via active constellation extension"". *IEEE Trans. Broadcasting*, pages pp. 258–268, Sep. 2003.

[14] Z.Latinovic M. Tan and Y.Bar-Ness. "STBC MIMO-OFDM Peak Power Reduction by Cross-Antenna Rotation and Inversion". *IEEE commun. Lett.*, 9:592–594, Jul. 2005.

[15] Branka Vucetic and Jinhong Yuan. "Space-time coding".

[16] Masound Olfat Weifeng Su, Zolan Safar and K. J. Ray Liu. "Obtaining Full-Diversity Space-Frequency Codes From Space-Time Codes via Mapping". *IEEE Transaction on Signal Processing*, 51:2905–2916, 2003.

[17] B. Lu and X. Wang. "Space-time code design in OFDM systems". *Proc. Globecom.*, 2:1000–1004, 2000.

[18] R.G. Gallager. "Low density parity check codes". *IRE Trans. Inform. Theory*, 8(1):pp. 21–28, Jan 1962.

[19] J.Speidel S.ten Brink and R.Yan. "Iterative demapping and decoding for multi-level modulation". *in Proc. GLOBECOM*, pages 579–584, Nov. 1998.

[20] Xiaodong Wang Ben Lu and Krishna R. Narayanan. "LDPC-Based Space-Time Coded OFDM Systems Over Correlated Fading Channels: Performance Analysis and Receiver Design". *IEEE transactions on communication*, 50:pp. 74–88, Jan. 2002.

[21] Alexei Ashikhmin Stephan ten Brink, Gerhard Kramer. "Design of Low-Density Parity-Check Codes for Modulation and Detecton". *IEEE transactions on communication*, 52:670–677, Apr. 2004.

[22] Guosen Yue Ben Lu and Xiaodong Wang. "Performance Analysis and Design Optimization of LDPC-Coded MIMO OFDM Systems". *IEEE transactions on signal processing*, 52:pp. 348–361, Feb. 2004.

[23] Joon Hyun Sung John R. Barry Steven W. McLaughlin Jeongseok Ha, Apurva N. Mody and Gordon L. Stuber. "LDPC Coded OFDM with Alamouti/SVD Diversity Technique".

[24] G. Stuber. "Priciples of Mobile Communication". 2001.

[25] Elton Deng. "Unitary Transform of Time-Shifted OFDM Blocks to Reduce PAPR". *PhD thesis*, 2007.

[26] C. Tellambura. "Phase optimisation criterion for reducing peak-to-average power ratio in OFDM". *Elect. Lett.*, pages 169–170, Jan. 1998.

[27] Yuhung Lo. "A Time-Domain PAPR Reduction Scheme for Coded MIMO OFDM"". *Master thesis*, 2007.